University of Nebraska - Lincoln

DigitalCommons@University of Nebraska - Lincoln

Faculty Publications, Department of Physics and Astronomy

Research Papers in Physics and Astronomy

2016

A time-implicit numerical method and benchmarks for the relativistic Vlasov–Ampere equations

Michael Carrié
University of Nebraska-Lincoln, mcarrie2@unl.edu

Bradley Allan Shadwick
University of Nebraska-Lincoln, shadwick@unl.edu

Follow this and additional works at: http://digitalcommons.unl.edu/physicsfacpub

A time-implicit numerical method and benchmarks for the relativistic Vlasov–Ampere equations

Michael Carrié[a)] and B. A. Shadwick[b)]

Department of Physics and Astronomy, University of Nebraska-Lincoln, Lincoln, Nebraska 68588, USA

We present a time-implicit numerical method to solve the relativistic Vlasov–Ampere system of equations on a two dimensional phase space grid. The time-splitting algorithm we use allows the generalization of the work presented here to higher dimensions keeping the linear aspect of the resulting discrete set of equations. The implicit method is benchmarked against linear theory results for the relativistic Landau damping for which analytical expressions using the Maxwell-Jüttner distribution function are derived. We note that, independently from the shape of the distribution function, the relativistic treatment features collective behaviours that do not exist in the nonrelativistic case. The numerical study of the relativistic two-stream instability completes the set of benchmarking tests. © *2016 AIP Publishing LLC*. [http://dx.doi.org/10.1063/1.4938035]

I. INTRODUCTION

An accurate treatment of the phase space dynamics is of fundamental importance to a broad range of relativistic plasma physics topics, including laser-based particle accelerators and radiation sources.[1,2] The dynamics in this context is governed by the Vlasov–Maxwell system of equations. Obtaining numerical solutions of this system, even in the simplest electrostatic case, presents some difficulties. For example, the nonlinear dependence of the relativistic factor on momentum requires advanced numerical methods when using a semi-Lagrangian method.[3] Eulerian phase space methods are attractive relative to macro-particle models due to the absence of effects related to sampling noise[4–7] and, at least in some circumstances, there is evidence that Eulerian methods can be more computationally efficient.[8]

Here, we restrict our attention to one spatial dimension, i.e., two phase space dimensions. While this restriction eliminates physics associated with magnetic field generation, it provides for a convenient setting for analyzing and benchmarking our proposed numerical method. Although there are drawbacks in adopting a purely electrostatic representation to study phase space dynamics, a one-dimensional, relativistic plasma response has been widely used in the literature to analyse a wide range of phenomena (see, for example, Refs. 9–22).

We consider a purely Eulerian approach (i.e., we solve for the distribution function on a phase space grid) with an implicit time-advance. To avoid solving a large nonlinear system of equations in the time-advance, operator splitting is used to convert the discrete equations into a set of low-bandwidth, linear systems. The implicit time-stepping results in unconditional numerical stability, and thus, the time-step is only constrained by accuracy considerations. Given the significant resources (computational and development) required to explore new Eulerian solvers, it is appropriate to begin the analysis of new algorithms in one spatial dimension; good performance in one spatial dimension, of course,

does not necessarily imply this performance will carry over to higher dimensions. Poor 1-D performance of an algorithm, however, would be a contraindication to pursuing a higher dimensional implementation. The extension of this method to high dimensional systems is straightforward (CPU and memory usage aside): additional splittings for the Vlasov equation must be introduced for each dimension, but at each level, the operators have the same structure as in the one dimensional case. (Of course, Ampere's law must be replaced by the full Maxwell equations, which can also be handled with operator splitting and an implicit time-advance.)

The paper is organized as follows. In Sec. II, we outline the Vlasov–Ampere equations and examine the linearized system. In Secs. III and IV, we survey the relevant phenomenology of the relativistic Vlasov–Ampere system. In Sec. V, we present our time-implicit numerical method, and in Sec. VI, we present benchmarks of our algorithm using various results from Secs. III and IV. We finally conclude the paper in Sec. VII.

II. THE 1D VLASOV-AMPERE SYSTEM OF EQUATIONS

We consider a one-dimensional (i.e., a two-dimensional phase-space), spatially periodic, relativistic plasma with a single mobile species of charge q and mass m and a fixed, neutralizing background of density n_0. While it is possible to express the distribution function in terms of position and velocity, it is more natural to use position and momentum (in which case the distribution function is a relativistic scalar[23]). If the plasma is sufficiently tenuous, the distribution function for the mobile species, $f(x, p, t)$, obeys the Vlasov equation

$$\frac{\partial f}{\partial t} + \frac{p}{m\gamma} \frac{\partial f}{\partial x} + q E \frac{\partial f}{\partial p} = 0, \tag{1}$$

where $\gamma = \sqrt{1 + p^2/m^2 c^2}$ is the usual Lorentz factor, c is the speed of light, and E is the electric field satisfying Ampere's law

$$\frac{\partial E}{\partial t} = -4\pi J \tag{2}$$

with current density J defined by

a)Electronic mail: mcarrie2@unl.edu
b)Electronic mail: shadwick@mailaps.org

$$J = q \int_{-\infty}^{+\infty} \frac{p}{m\gamma} f \, dp. \qquad (3)$$

We consider a spatially uniform equilibrium distribution $f^{(0)}(p)$ and examine first-order departures from equilibrium, $f^{(1)}$ and $E^{(1)}$. Assuming first-order quantities vary as $e^{i(kx-\omega t)}$ and defining $v = p/m\gamma$, the linearization of (1), (2), and (3) formally matches the nonrelativistic calculation,[24] ultimately yielding the dispersion relation

$$\epsilon(\omega, k) E^{(1)} = 0 \qquad (4)$$

with the plasma dielectric function given by

$$\epsilon(\omega, k) = 1 + \frac{m\,\omega_p^2}{k^2} \int_{-\infty}^{+\infty} \frac{1}{v_p - v} \frac{df_{eq}}{dp} \, dp, \qquad (5)$$

where $\omega_p^2 = 4\pi n_0 q^2/m$, $v_p = \omega/k$, and f_{eq} is defined by $f^{(0)} = n_0 f_{eq}$. Normal modes of the system must satisfy $\epsilon(\omega, k) = 0$. For $\text{Im}\,\omega \neq 0$, the integral in (5) is unambiguous. Using (A4), we have

$$\epsilon(\omega, k) = 1 - \frac{m\,\omega_p^2}{k^2} \text{P} \int \frac{1}{v - v_p} \frac{df_{eq}}{dp} \, dp$$
$$\mp i\pi \frac{m^2 \omega_p^2 \gamma_p^3}{k^2} \frac{df_{eq}}{dp}\bigg|_{p=\gamma_p v_p}, \quad \text{Im}\,\omega \to 0^{\pm}, \qquad (6)$$

where $\gamma_p = 1/\sqrt{1 - v_p^2/c^2}$ and P denotes the principal part. For the purpose of finding normal modes, this sign difference is immaterial, and the embedded neutral modes (Case class 1c[25]) satisfy $\text{Re}\,\epsilon = 0$. In the non-relativistic case, the existence of a neutral mode requires that the mode phase velocity corresponds to a critical point of the equilibrium distribution function.[25,26] In the relativistic case, as can be seen from (5), there is no singularity in the integrand for $\text{Im}\,\omega = 0$ provided $v_p \geq c$ (since all particle speeds must, of course, be below c). Thus, the existence of superluminal neutral modes is generic in the relativistic case.

In addition to the normal modes of the system, the time-asymptotic behaviour of the initial-value problem can also yield wake-like solutions.[27,28] As in the non-relativistic case, this asymptotic behaviour is governed by roots in the lower half-plane of the analytically continued dielectric function, $\Xi(\omega, k)$. Following (A5), we have

$$\Xi(\omega, k) = \epsilon(\omega, k) - \begin{cases} 0, & \omega_i \geq 0, \\ 2\pi i \dfrac{m^2 \omega_p^2 \gamma_p^3}{k^2} \dfrac{df_{eq}}{dp}\bigg|_{p=\gamma_p v_p}, & \omega_i < 0. \end{cases} \qquad (7)$$

Roots of $\Xi(\omega, k)$ in the lower half-plane give the Landau "quasi-modes" while roots in the upper half-plane (including the axis), which are also roots of $\epsilon(\omega, k)$, correspond to true normal modes. Complex roots, of course, come in conjugate pairs; for each unstable mode, there is a decaying mode corresponding to a root of $\epsilon(\omega, k)$ in the lower half-plane.

III. MONOTONIC EQUILIBRIUM

We begin our analysis of solutions of the dispersion relation by considering monotonic equilibria, in particular, the Maxwell–Jüttner distribution function[23]

$$f_{eq}(p) = \frac{1}{2mc\,K_1(\mu)} e^{-\mu\gamma}, \qquad (8)$$

where $\mu = mc^2/T$, T is the temperature, and K_1 is the modified Bessel function of the second kind.[29] It proves beneficial to introduce the following normalized quantities:

$$\begin{aligned} \Omega &= \frac{\omega}{\omega_p}, \\ K &= \frac{kc}{\omega_p}, \\ N &= \frac{kc}{\omega} = \frac{K}{\Omega} = \frac{c}{v_p}, \end{aligned} \qquad (9)$$

where v_p is the wave phase velocity and N is the refractive index. By splitting the integral in (5) into positive and negative momentum parts and transforming the integration variable by $p = \pm mc\sqrt{\gamma^2 - 1}$, the dielectric function can be written as

$$\epsilon(\omega, k) = 1 - \frac{\mu}{\Omega^2 K_1(\mu)} \int_1^\infty \frac{\gamma\sqrt{\gamma^2 - 1}}{\gamma^2(1 - N^2) + N^2} e^{-\mu\gamma} \, d\gamma. \quad (10)$$

The linear stability of the equilibrium (8) can be easily established through the relativistic version of the Penrose criterion.[30] As a result, the only possible solutions of (4) must correspond to $\omega_i = 0$, i.e., only neutral mode solutions exist. For $\text{Re}\,N \leq 1$, the integrand is non-singular for all N and ϵ is analytic and $\text{Im}\,\epsilon \to 0$ as $\text{Im}\,\omega \to 0$. For $\text{Re}\,N > 1$, the integrand has a pole when $\text{Im}\,N = 0$ and $\text{Im}\,\epsilon$ has a discontinuity as $\text{Im}\,\omega \to 0$. Thus neutral modes can exist only for $N \leq 1$. For $\text{Re}\,N \leq 1$, ϵ is analytic, thus $\Xi = \epsilon$ and quasi-modes are excluded for $\text{Re}\,N \leq 1$. Using (10), (A3), and (A4), we have

$$\Xi(\omega, k) = 1 - \frac{1}{\Omega^2} \frac{\mu}{K_1(\mu)} \times \begin{cases} \displaystyle\int_1^\infty \frac{e^{-\mu\gamma}\gamma\sqrt{\gamma^2 - 1}}{\gamma^2(1 - N^2) + N^2} \, d\gamma, & \text{Im}\,\Omega > 0, \\[4mm] \text{P}\displaystyle\int_1^\infty \frac{e^{-\mu\gamma}\gamma\sqrt{\gamma^2 - 1}}{\gamma^2(1 - N^2) + N^2} \, d\gamma - i\frac{\pi}{2} \frac{e^{-\mu\sqrt{N^2/(N^2 - 1)}}}{(N^2 - 1)^{3/2}}, & \text{Im}\,\Omega = 0, \\[4mm] \displaystyle\int_1^\infty \frac{e^{-\mu\gamma}\gamma\sqrt{\gamma^2 - 1}}{\gamma^2(1 - N^2) + N^2} \, d\gamma - i\pi\frac{e^{-\mu\sqrt{N^2/(N^2 - 1)}}}{(N^2 - 1)^{3/2}}, & \text{Im}\,\Omega < 0. \end{cases} \qquad (11)$$

This result can also be obtained from (7) using the same variable transformation leading to (10).

A. Neutral modes

First consider $N^2 = 1$ for which $v_p = c$ and (10) becomes

$$\epsilon(\omega, k) = 1 - \frac{1}{\Omega^2} \frac{\mu}{K_1(\mu)} \int_1^\infty e^{-\mu\gamma} \gamma \sqrt{\gamma^2 - 1} \, d\gamma. \quad (12)$$

Using the identity[29]

$$\int_1^\infty e^{-\mu\gamma} \gamma \sqrt{\gamma^2 - 1} \, d\gamma = \frac{K_2(\mu)}{\mu}, \quad (13)$$

we obtain

$$\Omega^2 = \frac{K_2(\mu)}{K_1(\mu)}. \quad (14)$$

This leads to a temperature dependent condition on the initial wave vector perturbation

$$k_c = \frac{\omega_p}{c} \sqrt{\frac{K_2(\mu)}{K_1(\mu)}}, \quad (15)$$

corresponding to the transition between superluminal modes and subluminal quasi-modes.

From (10), for real Ω, it is easy to show that $d\Omega/dN > 0$ implying $dk/dN > 0$ and thus for $N < 1$ (i.e., for $v_p > c$), $k < k_c$. Particles cannot interact resonantly with the wave, and there is no net energy transfer between particles and the wave. This is the main difference with the non-relativistic case where monotonic equilibria generically only support quasi-modes. In the non-relativistic case, there is no upper bound for the particle speed, and the wave-particle resonance is generally always present.

B. Quasi-modes

Quasi-modes are solutions of the analytically continued dielectric function, $\Xi(\omega, k)$, with $\text{Im}\,\omega < 0$. As we discussed above, this requires $\text{Re}\,N > 1$, and thus, quasi-modes will have wavenumbers greater than k_c. It does not appear possible to evaluate (11) in terms of elementary functions. To evaluate (11) numerically, we restrict the interval of integration to $[0, 1]$ by introducing a new variable $\gamma = 1 - 4/\mu \log[\sin(\pi\nu/2)]$.[31] The domain of integration is divided into 100 subdomains on which a 7-point Gaussian quadrature is applied. We show in Fig. 1 the real and imaginary parts solutions of $\Xi(\omega, k) = 0$ for different values of the perturbation wave number K and equilibrium temperature T.

IV. NON-MONOTONIC EQUILIBRIUM

In one dimension, only longitudinal instabilities can be excited whereas other instabilities with directions orthogonal to the direction of propagation could have more detrimental effects on the wave or beam propagation properties (as it is the case in the inertial confinement fusion (ICF) context[32]). Although studying a relativistic system without including
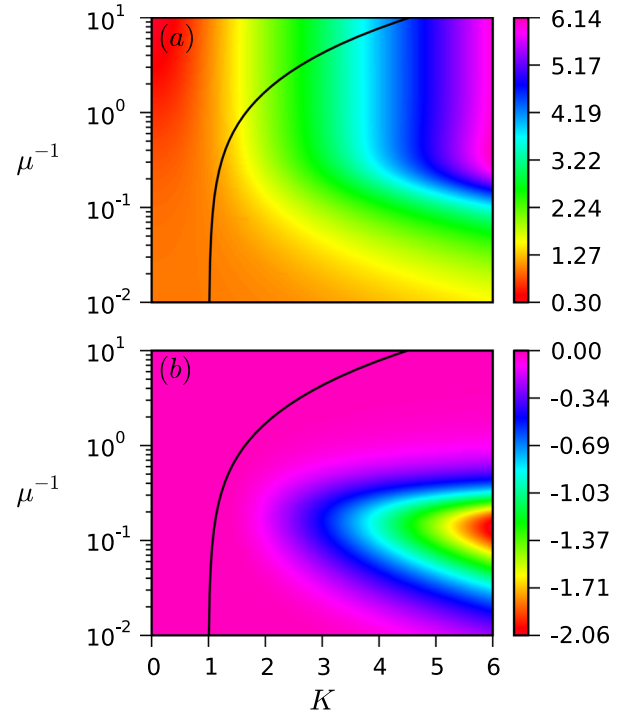

FIG. 1. Solutions of the dispersion relation $\Xi = 0$ as a function of K and temperature: (a) $\text{Re}\,\Omega$ and (b) $\text{Im}\,\Omega$. The black line denotes the transition between superluminal neutral modes and subluminal quasi-modes.

magnetic fields is questionable, it provides an excellent framework to benchmark numerical methods. It is in this vein that we consider the relativistic two-stream instability. To describe the relativistic two-stream equilibrium in the laboratory frame, we use two shifted Maxwell–Jüttner distributions with both beams having the same magnitude of the bulk momentum and temperature

$$f_{\text{eq}}(p) = \frac{1}{4mcK_1(\mu)} \left[e^{-\mu\sqrt{1+(p-p_0)^2/m^2c^2}} + e^{-\mu\sqrt{1+(p+p_0)^2/m^2c^2}} \right]. \quad (16)$$

(There are other, physically reasonable, relativistic two-stream equilibria; see Refs. 32 and 33.) To find the stability condition, we apply the relativistic Penrose criterion[30]

$$\int_{-\infty}^{+\infty} \frac{df_{\text{eq}}}{dp} \frac{1}{p/m\gamma - v_{\text{min}}} \, dp > 0, \quad (17)$$

where v_{min} corresponds to the local minimum of f_{eq} ($v_{\text{min}} = 0$ in our case) to our two-stream equilibrium, (16). The integral in (17) has a removable singularity at $p = 0$ and can be easily computed numerically. Fig. 2 shows the region of parameters space where the instability can develop. As in the non-relativistic case, the separation between the streams determines stability; for a given temperature, once the separation exceeds a threshold value, the system becomes unstable.

The stable region resembles the monotonic equilibrium case; we have superluminal neutral modes and (damped) quasi-modes. In the unstable region, in addition to the neutral and quasi-modes, we have (one or more) exponentially growing and damped modes. In this regime, the growing modes dominate the plasma response. Subsequently, we
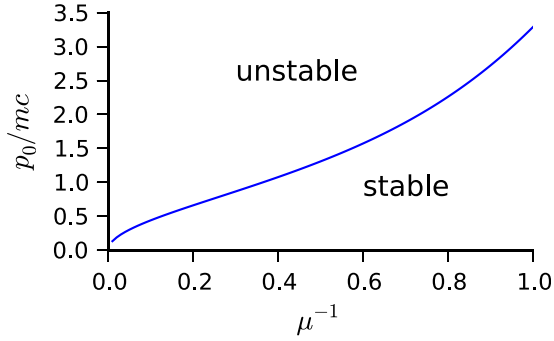
FIG. 2. Instability region for the equilibrium (16).

FIG. 4. Growth rate ImΩ as a function of K for $\mu^{-1} = 0.01$ and various bulk momenta. The crosses indicate numerical results of Sec. V.

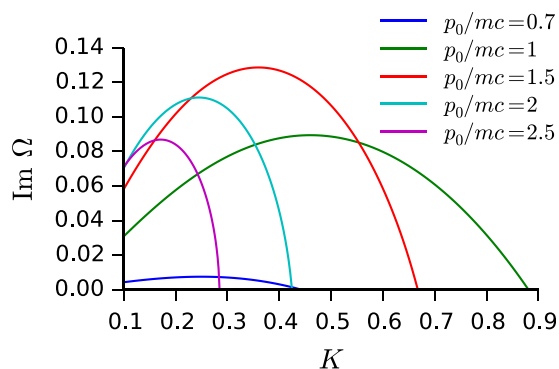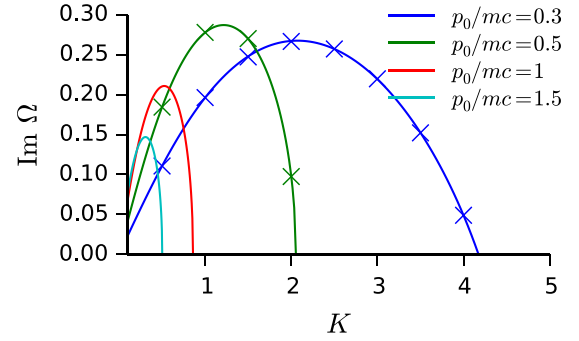focus on the unstable modes, looking for purely imaginary solutions of $\epsilon = 0$.

Since our equilibrium is an even function of p, we can write the dielectric function, (5), as

$$\epsilon(\omega, k) = 1 + \frac{2mc}{\Omega^2} \int_0^\infty \frac{p\sqrt{m^2c^2 + p^2}}{p^2(1 - N^2) + m^2c^2} \frac{df_{\mathrm{eq}}}{dp} \, dp. \quad (18)$$

For ImΩ > 0, (18) can be evaluated straightforwardly numerically. An exhaustive study of the growth rate involves a three dimensional parameter space (K, μ, and p_0). Here, we consider parameters values relevant to ICF: temperatures of a few hundred of keV and bulk energy of the order of 1 MeV.

In Fig. 3, we plot the growth rate for different bulk momenta and a temperature of $T \approx 100$ keV. The maximum growth rate (as a function of K) depends on p_0, having a peak for $p_0 = 1.5\,mc$. For a lower temperature, $T \approx 5$ keV (see Fig. 4), the growth rate has its maximum at lower bulk momentum and peaks around $K = 1$, i.e., for perturbation of the order of the electron plasma wavelength.

For electron distribution parameters relevant to ICF, there is an intermediate situation where the instability can develop. The growth rates are maximum for low temperatures, and low bulk momentum and the instability can be suppressed by increasing the temperature (bulk width) and/or the bulk velocity. We also note that for these range of parameters, collisions (ignored here) can play an important role by dissipating some of the electron kinetic energy having the effect of reducing the instability growth rate.[32]

FIG. 3. Growth rate ImΩ as a function of K for a fixed temperature $\mu^{-1} = 0.2$ and different bulk momenta.

V. NUMERICAL ALGORITHM

Here, we consider a purely Eulerian numerical solution of (1) and (2), that is, we will solve (1) on a phase space grid without recourse to characteristics. This method is the relativistic extension of a method we developed for the Vlasov–Poisson system.[34–36] We construct a regular, uniform grid of points (x_k, p_j) over phase space of size $N_x \times N_p$ with $x_k = x_1 + (k-1)\Delta x$, $k = 1, \ldots, N_x$, where $\Delta x = (x_{N_x} - x_1)/(N_x - 1)$ and $p_j = p_1 + (j-1)\Delta p$, $j = 1, \ldots, N_p$, where $\Delta p = (p_{N_p} - p_1)/(N_p - 1)$. Periodicity in x is imposed by identifying $x_{N_x} + \Delta x$ with x_1 and consequently $x_1 - \Delta x$ with x_{N_x-1}. The periodicity length, L, of the spatial domain is then $L = x_{N_x} + \Delta x - x_1$. The momentum grid is assumed to contain the support of f; thus, we take $f(x, p_1 - \Delta p, t) = 0 = f(x, p_{N_p} + \Delta p, t)$. We take a fixed time-step Δt and put $t_n = t_1 + (n-1)\Delta t$. Without loss of generality, we may assume $t_1 = 0$. In what follows, we take f_{kj}^n to be the numerical approximation of $f(x_k, p_j, t_n)$. We use the Crank–Nicolson time-centered scheme[37] with phase-space derivatives represented by second-order central differences

$$\left.\frac{\partial f}{\partial t}\right|_{x_k, p_j}^{t_{n+1/2}} = \frac{f_{kj}^{n+1} - f_{kj}^n}{\Delta t} + \mathcal{O}(\Delta t^2), \quad (19a)$$

$$\left.\frac{\partial f}{\partial x}\right|_{x_k, p_j}^{t_{n+1/2}} = \frac{1}{2}\left(\frac{f_{k+1j}^{n+1} - f_{k-1j}^{n+1}}{2\Delta x} + \frac{f_{k+1j}^n - f_{k-1j}^n}{2\Delta x}\right) + \mathcal{O}(\Delta x^2) + \mathcal{O}(\Delta t^2), \quad (19b)$$

$$\left.\frac{\partial f}{\partial p}\right|_{x_k, p_j}^{t_{n+1/2}} = \frac{1}{2}\left(\frac{f_{kj+1}^{n+1} - f_{kj-1}^{n+1}}{2\Delta p} + \frac{f_{kj+1}^n - f_{kj-1}^n}{2\Delta p}\right) + \mathcal{O}(\Delta p^2) + \mathcal{O}(\Delta t^2), \quad (19c)$$

$$\left.f\right|_{x_k, v_j}^{t_{n+1/2}} = \frac{1}{2}\left(f_{kj}^{n+1} + f_{kj}^n\right) + \mathcal{O}(\Delta t^2). \quad (19d)$$

Applying this discretization directly to (1) and (2) leads to a large nonlinear system of equations that must be solved at each time step. The size of the system precludes the use of direct methods even in one spatial dimension.

An alternative is to split the Vlasov–Ampere equations into

$$\frac{\partial f}{\partial t} + \frac{p}{m\gamma}\frac{\partial f}{\partial x} = 0,$$
$$\frac{\partial E}{\partial t} = 0, \quad (20a)$$

$$\frac{\partial f}{\partial t} = 0,$$
$$\frac{\partial E}{\partial t} = -4\pi q \int \frac{p}{m\,\gamma} f\, dp \tag{20b}$$

and

$$\frac{\partial f}{\partial t} + q\, E\, \frac{\partial f}{\partial p} = 0,$$
$$\frac{\partial E}{\partial t} = 0, \tag{20c}$$

which has the effect of removing the nonlinearity. This is essentially the same splitting used by Cheng and Knorr[38] in their semi-Lagrangian method, by Schumer and Holloway[39] in their Hermite spectral algorithm, and by Sircombe and Arber[40] in constructing explicit Eulerian methods. To second order accuracy in time, we can compute the time evolution using the symmetric Strang approach.[41] Let the operators $U_1(\Delta t)$, $U_2(\Delta t)$, and $U_3(\Delta t)$ give the evolution of f and E from t to $t + \Delta t$ corresponding to (20a), (20b), and (20c), respectively. Provided the U_i are at least second-order accurate in Δt (or first-order accurate and time-reversible[42]), the evolution corresponding to (1) and (2) from t to $t + \Delta t$ is given by

$$U_1(\Delta t/2)\, U_2(\Delta t/2)\, U_3(\Delta t)\, U_2(\Delta t/2)\, U_1(\Delta t/2), \tag{21}$$

accurate to second order in Δt. We apply the Crank–Nicolson discretization (19) to (20) to obtain the update operators U_i. In each case, it is at most necessary to solve a tri-diagonal linear system of equations, for which fast direct methods exist.[43] This scheme conserves the total particle number, momentum, and enstrophy, $\int f^2 dx\, dp$, to machine precision.[34–36] The total energy is conserved consistent with the second-order truncation error of the method. Further, as in the non-relativistic case,[34–36] the method is unconditionally stable; thus, the time step is only limited by accuracy considerations.

Of importance when solving Vlasov equation on a phase space grid is ensuring positivity of the distribution function. Our numerical scheme does not include any dissipation mechanisms. As a consequence, when the spatial gradients of the distribution function reach the grid size level, oscillations are produced in the solution, giving rise to negative values of f. The generation of negative values of f is not unique to our method and has been observed in numerous studies using a phase-space grid.[38,44,45]

The consequences of these negative values appear negligible compared to other numerical artefacts and does not influence the dynamics of the system.[44] Schemes for maintaining positivity are under active investigation and require the use of techniques adapted from the computational fluid dynamics community. These methods bring with them the disadvantage of not conserving fundamental invariant except the particle number.[34–36,46] There is ultimately a trade-off between positivity and invariant conservation depending on the physics problem being studied.

VI. EXAMPLES

All computations are performed in normalized variables: the plasma frequency is use to set temporal and spatial scales; momenta are normalized to mc; the electric field is normalized to $mc\omega_p/e$; and the background density n_0 scales out. Oscillations are excited by initializing the distribution function with a spatial modulation of wave number k

$$f(t=0,x,p) = n_0(1 + A\cos kx)f_{\rm eq}(p) \tag{22}$$

with $k = 2\pi n/L$, where n is an integer. We identify $f^{(1)} = A\, n_0 \cos(kx) f_{\rm eq}(p)$. We use a simulation box of $[0, 4\pi] \times [-5, 5]$ in the x and p directions, respectively (in normalized units). For the following simulation results, unless specified otherwise, we use a phase space grid $\omega_p \Delta t = 0.1$, $\Delta p = 0.01\, mc$, and $\omega_p \Delta x = 0.0245\, c$ ($N_x = 512$ and $N_p = 1000$).

A. Monotonic equilibrium

We solve the linearized system of equations taking a Maxwell-Jüttner equilibrium distribution function with $A = 0.1$. In Fig. 5, we plot the time evolution of the electric field for $K = 0.5$ and $T = 0.1\, mc^2$ corresponding to an undamped mode. The linear theory gives $\omega = 0.9645\, \omega_p$. The oscillation frequency of the numerical solution agrees to the third digit with this set of grid parameters. For this temperature, according to expression (15), the transition between superluminal and subluminal mode is given by $k_c\, c \approx 1.074\, \omega_p$.

Fig. 6 shows the solution for the same temperature $T = 0.1$ but with $K = 2$, which corresponds to a damped quasi-mode. The linear theory gives a damping rate $\omega_i = -0.098\, \omega_p$ and a frequency $\omega_r = 1.468\, \omega_p$. From the numerical solution, we find $\omega_i = -0.097\, \omega_p$ and $\omega_r = 1.467\, \omega_p$. Since our method does not introduce any noise (numerical collisions or dissipation), we can observe the decay over 12 decades. As in the non-relativistic case, we can define a recurrence time for the free streaming case given by $\omega_p\, t_r = (2\pi/k)\,\Delta p$. With this set of parameters, we have $\omega_p\, t_r = 314.15$, and we observe the maximum of the electric recurrence around $\omega_p t = 317$.

In the Laplace transform treatment of the relativistic initial value problem, in addition to contributions to the electric field from poles (which give rise to the usual quasi-modes), there are contributions from branch cuts due to the upper bound on particle velocity. The asymptotic structure of the electric field due to these branch cuts was first determined by Godfrey et al.[9] and later refined by Sartori and Coppa.[11] This
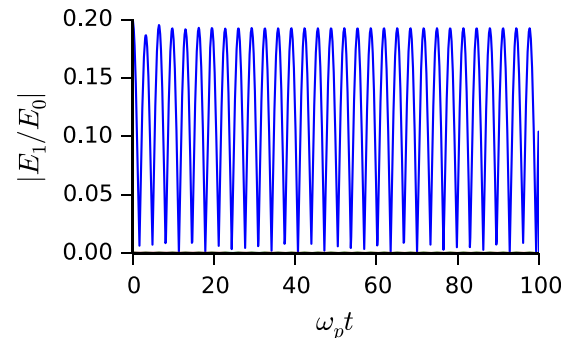

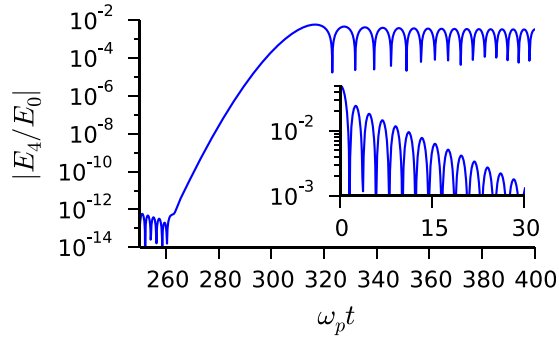FIG. 5. Fundamental electric field mode for $A = 0.1$, $K = 0.5$, and $T = 0.1\, mc^2$.

FIG. 6. Fundamental electric field mode for $A = 0.1$, $K = 2$, and $T = 0.1\, mc^2$.

behavior makes for a sensitive benchmark as the electric field must be followed for a large number of oscillations. This phenomenon appears inaccessible to macro-particle methods[5,6] as unmanageably large numbers of macroparticles would be necessary to keep sampling noise low enough. To see this effect, it is necessary to chose k and T such that the quasi-mode solution is damped very rapidly and the branch cut contribution is non-negligible. To this end, we take $K = 8$, $T = 0.2\, mc^2$ and solve the linearised system of equations with $\omega_p \Delta t = 0.015$, $\Delta p = 0.005\, mc$, and $\omega_p \Delta x = 0.0245\, c$. For these parameters, the quasi-mode has $\omega_r = 7.903\, \omega_p$ and $\omega_i = -2.576\, \omega_p$ and thus decays rapidly. The amplitude of the electric field decays as[9,11]

$$E \propto t^{1/6} \exp\left[-\frac{3\sqrt{3}}{4}\left(\mu^2 k\, c\, t\right)^{1/3}\right]. \quad (23)$$

The electric field from the numerical solution is shown in Fig. 7 (blue line) along with amplitude given by (23) (red line). We see that very early in the calculation, the system enters the time-asymptotic behavior arising from the branch cut and there is an excellent agreement between the numerical solution and the amplitude (23).

Sartori and Coppa[11] provide a corrected expression for the full time-dependence of the electric field [cf. (19) in Ref. 11]

$$E \propto t^{1/6} \exp\left[-\frac{3\sqrt{3}}{4}\left(\mu^2 kc\, t\right)^{1/3}\right]$$
$$\times \sin\left[kc\, t - \frac{3}{4}\left(\mu^2 kc\, t\right)^{1/3} + \frac{\pi}{12}\right]. \quad (24)$$
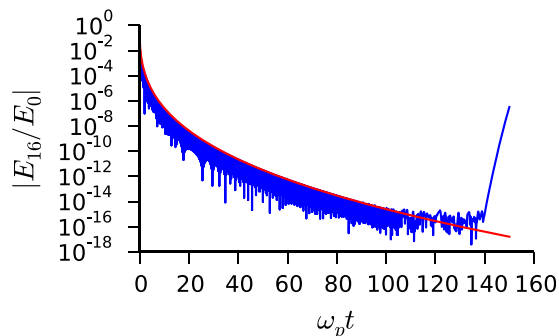

FIG. 7. Electric field for $A = 0.1$, $kc/\omega_p = 8$ and $T/mc^2 = 0.2$ (blue) along with the amplitude given by (23) (red).
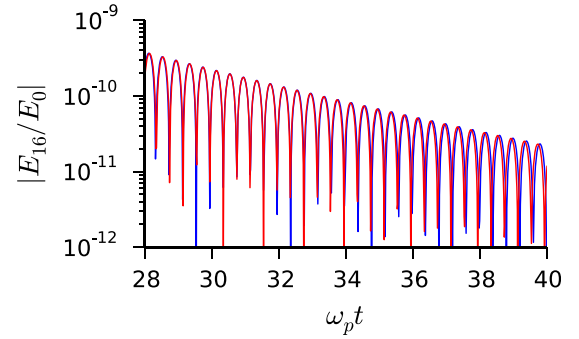

FIG. 8. A comparison or the numerical solution (blue) with (24) (red). The section shown is representative of the electric field behavior over the full time interval.

Comparing this to our numerical solution, we observe a phase error as can be seen in Fig. 8. To understand the origin of this discrepancy, we assume the time dependence derived by Sartori to be correct and attempt to fit the numerical solution to

$$E = C\, t^{1/6}\, e^{-p_1 t^{1/3}} \sin\left(p_2\, t - p_3\, t^{1/3} + p_4\right). \quad (25)$$

The results of a least-squares fit (except for C which is uninteresting) are shown in Table I along with the corresponding values from (24). Fig. 9 shows the electric field from the numerical solution and the result of fitting (25). We have repeated this procedure for different initial wavenumbers and equilibrium temperatures, and in all cases, we find the phase constant to be approximately 1.9. These results strongly suggest that the constant phase in (24) is incorrect. (Analytically determining the value of p_4 is beyond the scope of this work.)

B. Non-monotonic equilibrium

We conclude this section by considering the relativistic two-stream instability with the equilibrium distribution function (16). We take $p_0 = 0.5\, mc$, $T = 0.01\, /mc^2$, and $K = 1$ and compute the full nonlinear solution. The initial amplitude of the perturbation is set to $A = 10^{-6}$ to observe the linear growth during the first stage of the simulation. The linear theory gives $\omega_i = 0.277\, \omega_p$ compared to the value determined from the numerical solution of $0.276\, \omega_p$. After a period of exponential growth, the electric field saturates, and we observe a BGK mode as in the non-relativistic case. Fig. 10 shows the electron distribution function at the end of the simulation. Negative values are clearly visible, but they appear to be harmless with respect to the electric field evolution. We show in Fig. 4 the growth rate as a function of K obtained from numerical solutions for $T = 0.01\, /mc^2$ and various values of p_0. With this set of grid parameters, the

TABLE I. Result of a least-squares fit the numerical solution to (25) compared the coefficients in (23).

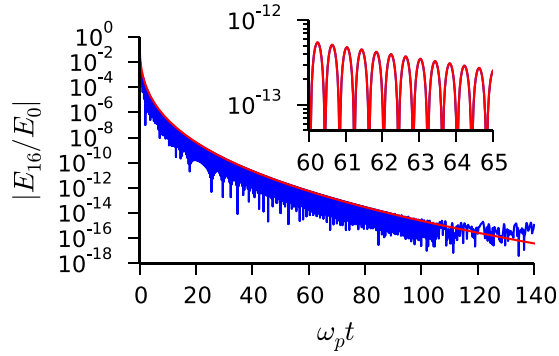|	p_1	p_2	p_3	p_4
Fit	7.54	7.94	4.39	1.92
(19) of Ref. 11	7.59	8.00	4.38	0.26

FIG. 9. Electric field for $A = 0.1$, $kc/\omega_p = 8$, and $T/mc^2 = 0.2$ (blue) along with the amplitude given by (23) (red). The inset shows the electric field from the numerical solution (blue) along with a least-squares fit to (25); see Table I.

relative error between theoretical and numerical growth rates is on the order of 10^{-3}.

VII. CONCLUSIONS

In this work, we extended a numerical method developed for the non-relativistic Vlasov–Ampere system to the relativistic case.[35,36] We applied our algorithm to both the full nonlinear system and to the linearized equations and found excellent agreement in a variety of benchmarks. While this algorithm is capable of producing negative values for the distribution function, these negative values did not significantly affect the evolution of the electric field. As long as no mechanism to maintain the distribution positivity is introduced (collisions, limiters, TVD methods, etc.), negative values can be expected when solving on a phase space grid. In the non-relativistic case, we have seen that attempts to prevent negative values of the distribution function introduce other errors on phase space that appear to be more detrimental than the negative values;[34–36] we expect this behavior to carry over to the relativistic case. We examined the long-time behavior of the electric field—possible only with an Eulerian numerical method—arising from a branch cut and identified a possible error in previously derived asymptotic expression[11] for the electric field. We plan to extend this algorithm to the electromagnetic case in four phase-space dimensions for studying laser-plasma interactions and will report those results in due course.
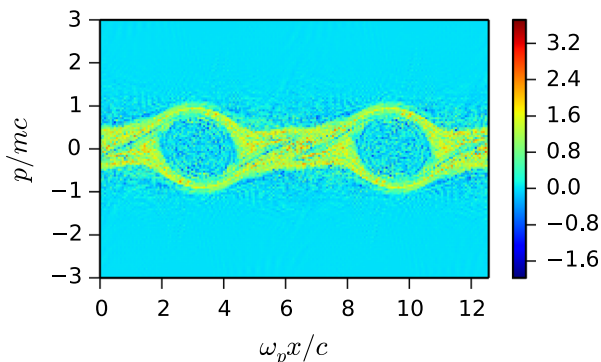

FIG. 10. Two-stream instability: electron distribution function at $\omega_p t = 100$ for $K = 1$, $T = 0.01\, mc^2$, and $p_0 = 0.5\, mc$.

APPENDIX: A SINGULAR INTEGRALS

For $y \in \mathbb{C}$ and $\mathrm{Im}\, y \neq 0$, and with rather generous restrictions on $\phi(x)$,[47] the integral

$$\psi(y) = \int dx\, \frac{\phi(x)}{x - y} \tag{A1}$$

is well-defined, analytic in the upper and lower half-planes, and[47]

$$\lim_{\mathrm{Im}\, y \to 0^\pm} \int dx\, \frac{\phi(x)}{x - y} = \mathrm{P} \int dx\, \frac{\phi(x)}{x - y} \pm i\,\pi\, \phi(y), \tag{A2}$$

where P denotes the principal part. (The domain of integration is immaterial as long as y is restricted to its interior.) Clearly, $\psi(y)$ has a jump as y crosses the real axis, and thus, ψ is not analytic in the plane. It is straightforward to analytically continue ψ into either the lower or upper half-plane. As a generalization, let $\alpha(x, y)$ have a simple root at $x = x_0$ for y real and consider

$$\int dx\, \frac{\phi(x)}{\alpha(x, y)} = \int dx\, \frac{1}{x - y} \left[\frac{x - y}{\alpha(x, y)}\, \phi(x) \right]. \tag{A3}$$

For $\mathrm{Im}\, y \neq 0$, the term in brackets is regular, while for $\mathrm{Im}\, y = 0$ it has a removable singularity at $x = y$. Under suitable conditions on ϕ and α, this integral is well-defined in the upper and lower planes and

$$\lim_{\mathrm{Im}\, y \to 0^\pm} \int dx\, \frac{\phi(x)}{\alpha(x, y)} = \mathrm{P} \int dv\, \frac{\phi(x)}{\alpha(x, y)} \pm i\,\pi\, \frac{\phi(x)}{\partial \alpha(x, y)/\partial x}\bigg|_{x = x_0}. \tag{A4}$$

We can construct the analytic continuation, Ψ, of (A3) from the upper to lower half plane as

$$\Psi(y) = \int dx\, \frac{\phi(x)}{\alpha(x, y)} + \begin{cases} 0, & \mathrm{Im}\, y \geq 0, \\[2mm] 2i\,\pi\, \dfrac{\phi(x)}{\partial \alpha(x, y)/\partial x}\bigg|_{x = x_0}, & \mathrm{Im}\, y < 0. \end{cases} \tag{A5}$$

[1]M. Murakami, Y. Hishikawa, S. Miyajima, Y. Okazaki, K. L. Sutherland, M. Abe, S. V. Bulanov, H. Daido, T. Z. Esirkepov, J. Koga, M. Yamagiwa, and T. Tajima, AIP Conf. Proc. **1024**, 275–300 (2008).
[2]S. Cipiccia, M. R. Islam, B. Ersfeld, R. P. Shanks, E. Brunetti, G. Vieux, X. Yang, R. C. Issac, S. M. Wiggins, G. H. Welsh, M.-P. Anania, D. Maneuski, R. Montgomery, G. Smith, M. Hoek, D. J. Hamilton, N. R. C. Lemos, D. Symes, P. P. Rajeev, V. O. Shea, J. M. Dias, and D. A. Jaroszynski, Nat. Phys. **7**, 867 (2011).
[3]M. Shoucri, Commun. Nonlinear Sci. Numer. Simul. **13**, 174 (2008).
[4]A. B. Langdon, J. Comput. Phys. **6**, 247 (1970).
[5]C. K. Birdsall and A. B. Langdon, *Plasma Physics via Computer Simulations*, Plasma Physics Series (Institute of Physics Publishing, Bristol, 1991).

[6]R. W. Hockney and J. W. Eastwood, *Computer Simulation Using Particles* (Taylor and Francis Group, New York, 1988).

[7]E. Cormier-Michel, B. A. Shadwick, C. G. R. Geddes, E. Esarey, C. B. Schroeder, and W. P. Leemans, Phys. Rev. E **78**, 016404 (2008).

[8]B. A. Shadwick, A. B. Stamm, and E. G. Evstatiev, Phys. Plasmas **21**, 055708 (2014).

[9]B. Godfrey, B. Newberger, and K. Taggart, IEEE Trans. Plasma Sci. **3**, 185 (1975).

[10]T. Katsouleas and W. B. Mori, Phys. Rev. Lett. **61**, 90 (1989).

[11]C. Sartori and G. G. M. Coppa, Phys. Plasmas **2**, 4049 (1995).

[12]A. G. Khachatryan, Phys. Plasmas **5**, 112 (1998).

[13]A. Ghizzo, P. Bertrand, J. Lebas, T. W. Johnston, and M. Shoucri, Phys. Plasmas **5**, 4041 (1998).

[14]F. Huot, A. Ghizzo, P. Bertrand, E. Sonnendrucker, and O. Coulaud, IEEE Trans. Plasma Sci. **28**, 1170 (2000).

[15]L. M. Gorbunov, P. Mora, and R. R. Ramazashvili, Phys. Rev. E **65**, 036401 (2002).

[16]B. Eliasson and P. K. Shukla, Phys. Plasmas **12**, 104501 (2005).

[17]B. A. Shadwick, G. M. Tarkenton, and E. H. Esarey, Phys. Rev. Lett. **93**, 175002 (2004).

[18]B. A. Shadwick, G. M. Tarkenton, E. Esarey, and C. B. Schroeder, Phys. Plasmas **12**, 056710 (2005).

[19]C. B. Schroeder, E. Esarey, B. A. Shadwick, and W. P. Leemans, Phys. Plasmas **13**, 033103 (2006).

[20]R. M. G. M. Trines and P. A. Norreys, Phys. Plasmas **13**, 123102 (2006).

[21]B. Eliasson and P. K. Shukla, Phys. Plasmas **14**, 056703 (2007).

[22]H. Zhang, S. Z. Wu, C. T. Zhou, S. P. Zhu, and X. T. He, Phys. Plasmas **20**, 092112 (2013).

[23]S. R. de Groot, W. A. van Leeuwen, and Ch. G. van Weert, *Relativistic Kinetic Theory: Principles and Applications* (North-Holland, New York, 1980).

[24]N. A. Krall and A. W. Trivelpiece, *Principles of Plasma Physics* (McGraw-Hill New York, 1973).

[25]K. M. Case, Phys. Fluids **21**, 249 (1978).

[26]B. A. Shadwick and P. J. Morrison, Phys. Lett. A **184**, 277 (1994).

[27]L. D. Landau, J. Phys. USSR **10**, 25 (1946); Sov. Phys. JETP **16**, 547 (1946).

[28]N. G. van Kampen and B. Felderhof, *Theoretical Methods in Plasma Physics* (North-Holland, Amsterdam, 1967).

[29]M. Abramowitz and I. A. Stegun, *Handbook of Mathematical Functions* (Dover, New York, 1965).

[30]R. Buschauer and G. Benford, Mon. Not. R. Astron. Soc. **179**, 99 (1977).

[31]J. Bergman and B. Eliasson, Phys. Plasmas **8**, 1482 (2001).

[32]L. A. Cottrill, A. B. Langdon, B. F. Lasinski, S. M. Lund, K. Molvig, M. Tabak, R. P. J. Town, and E. A. Williams, Phys. Plasmas **15**, 082108 (2008).

[33]M. Lazar, A. Stockem, and R. Schlickeiser, Open Plasma Phys. J. **3**, 138 (2010).

[34]M. Carrié and B. A. Shadwick, Bull. Am. Phys. Soc. **58**, 85 (2013).

[35]M. Carrié and B. A. Shadwick, "A time-implicit algorithm for solving the one-dimensional Vlasov-Poisson system of equations" (unpublished).

[36]M. Carrié and B. A. Shadwick, Bull. Am. Phys. Soc. **57**, 356 (2012).

[37]J. Crank and P. Nicolson, Math. Proc. Cambridge Philos. Soc. **43**, 50 (1947).

[38]C. Cheng and G. Knorr, J. Comput. Phys. **22**, 330 (1976).

[39]J. W. Schumer and J. P. Holloway, J. Comput. Phys. **144**, 626 (1998).

[40]N. Sircombe and T. Arber, J. Comput. Phys. **228**, 4773 (2009).

[41]G. Strang, SIAM J. Numer. Anal. **5**, 506 (1968).

[42]W. Kahan and R.-C. Li, Math. Comput. **66**, 1089 (1997).

[43]L. H. Thomas, Watson Scientific Computing Laboratory Report, "Elliptic Problems in Linear Differential Equations over a Network" (Columbia University, New York, 1949).

[44]T. Arber and R. Vann, J. Comput. Phys. **180**, 339 (2002).

[45]R. Heath, I. Gamba, P. Morrison, and C. Michler, J. Comput. Phys. **231**, 1140 (2012).

[46]N. Elkina and J. Büchner, J. Comput. Phys. **213**, 862 (2006).

[47]F. D. Gakhov, *Boundary Value Problems* (Dover, New York, 1990).